JOURNAL OF GUIDANCE, CONTROL, AND DYNAMICS
Vol. 20, No. 1, January–February 1997

Missile Autopilot Design Using a New Linear Time-Varying Control Technique

J. Jim Zhu and M. Christopher Mickle
Louisiana State University, Baton Rouge, Louisiana 70803-6430

Design and simulation case studies of a missile autopilot for angle of attack and normal acceleration tracking using a recently developed extended-mean assignment (EMA) control technique for linear time-varying (LTV) systems are presented. The EMA control technique is based on a new eigenvalue concept, called series D (SD) eigenvalue, for LTV systems. Closed-loop stability is achieved by the assignment of the extended-mean of these time-varying SD eigenvalues to the left-half complex plane in a way similar to the eigenvalue (pole) assignment technique for linear time-invariant systems. Salient features of the tracking controller include the following: 1) good tracking performance for arbitrary trajectories without scheduling of any constant design parameters throughout the entire Mach operating range; 2) time-varying EMA command, or pole locations, to improve tracking performance; 3) implementation of the inverse pitch dynamics using a static neural network; and 4) a time-varying bandwidth command shaping filter that effectively reduces the actuator rate while maintaining good tracking response for both smooth and abrupt guidance command trajectories. Although the autopilot was designed only for nominal aerodynamic coefficients, excellent performance was verified by simulation for ±50% variations in the aerodynamic coefficients.

Nomenclature

$C_m[\alpha, \delta, M]$	= pitch moment coefficient
$C_n[\alpha, \delta, M]$	= aerodynamic lift coefficient
D	= derivative operator, d/dt
$\mathcal{D}_a, \mathcal{D}_h$	= polynomial differential operator
$k_1(t), k_2(t)$	= time-varying feedback gains
$M(t)$	= Mach number
$q(t)$	= pitch rate, deg/s
$v(t)$	= tracking error control input
$\boldsymbol{x}(t)$	= state tracking error
$y(t)$	= normal acceleration tracking error
$z(t)$	= angle-of-attack tracking error
$\alpha(t)$	= angle of attack, deg
$\gamma_1(t), \gamma_2(t)$	= closed-loop series D (SD) eigenvalues
$\delta(t)$	= actual tail fin deflection, deg
$\delta_c(t)$	= commanded tail fin deflection, deg
$\eta_c(t)$	= commanded normal acceleration, g
$\eta_z(t)$	= actual normal acceleration, g
$\lambda_1(t), \lambda_2(t)$	= open-loop SD eigenvalues
$\bar{\boldsymbol{\xi}}, \bar{\delta}$	= nominal state trajectory and nominal control input, respectively
ξ_1, ξ_2	= state variables for α and q

I. Introduction

THIS paper presents design and simulation case studies of a missile autopilot using a recently developed extended-mean assignment (EMA) control technique for linear time-varying (LTV) systems. The EMA control technique is very similar to the conventional eigenvalue (pole) placement design for linear time-invariant (LTI) systems but is based on a new, time-varying series D eigenvalue (SD-eigenvalue) concept.[1–4] The autopilot is to control the nonlinear time-varying pitch-axis dynamics of a hypothetical tail-controlled missile, which has been used as a benchmark in a number of recent studies on nonlinear gain-scheduling design techniques.[5–7]

J. Jim Zhu received his M.S. (1984) in Control, M.A. (1986) in Mathematics, and Ph.D. (1989) in Control with an honor of Highest Academic Achievement from the University of Alabama in Huntsville. Zhu joined Louisiana State University in July 1990 and presently holds a joint appointment as Assistant Professor in the Department of Electrical and Computer Engineering, and Research Faculty in the Remote Sensing and Image Processing Laboratory. Zhu's main research area and contribution is in time-varying linear systems theory. His current research interests include time-varying linear and nonlinear dynamical and control systems theory with applications in flight control and signal processing. He is a Member of AIAA.

M. Christopher Mickle received a B.S. summa cum laude in Electrical Engineering from Lamar University in 1993 and an M.S. in Electrical Engineering from Louisiana State University in 1995. He is currently a doctoral candidate in the Department of Electrical and Computer Engineering, Louisiana State University. His research interests are in the areas of linear time-varying systems and nonlinear control systems with applications to flight control. Mickle is the recipient of the Louisiana State Board of Regents' Deans Fellowship in Engineering.

Received Dec. 27, 1995; revision received Aug. 22, 1996; accepted for publication Sept. 20, 1996.

The nonlinear pitch dynamics of the missile was rendered into an LTV system via the classical linearization along a nominal trajectory, and then operated on by a linear coordinate transformation to make it tractable by the EMA control technique. The problem of nonminimum phase zero dynamics of the normal acceleration (NA) tracking is effectively circumvented by mapping it algebraically to the angle-of-attack (AOA) tracking, which is of minimum phase. This technique can be viewed as a variant of the output redefinition approach introduced in Ref. 8.

A radical departure from the conventional design philosophy is that nonlinearity and time variance are not treated as nuisances, but purposely utilized to accomplish design objectives beyond the capability of LTI controllers. Salient features of the EMA tracking controller include 1) good tracking performance for arbitrary trajectories without scheduling of any constant design parameters throughout the entire Mach operating range, 2) time-varying EMA command, or pole locations to improve tracking performance, 3) implementation of the inverse pitch dynamics using a static neural network (NN), and 4) a time-varying bandwidth command shaping filter that effectively reduces the actuator rate while maintaining good tracking response for both smooth and abrupt trajectories. It is also noted that the EMA design technique presented here differs from the prototype presented in Ref. 4 in that the feedback control gains are synthesized directly from the desired closed-loop SD eigenvalues and the plant coefficients, bypassing the analysis of the open-loop SD eigenvalues.

In Sec. II, the design principle and procedure for EMA control by direct synthesis are presented for a generic second-order LTV plant. The results are readily extended to the general case of the nth-order LTV systems using the parallel D (PD) and SD spectral theory[2,3] and systematic controller design procedure[9] for LTV systems. Section III details the design and implementation of the EMA-based autopilot, including 1) the pitch dynamic model of the missile airframe, 2) EMA controller design for AOA tracking subsystem, 3) NA tracking via the AOA tracking subsystem by using an AOA state observer to estimate the AOA tracking error from that of the NA measurement, 4) the radial basis function (RBF) NN-based inverse plant implementation, 5) the time-varying EMA command logic, and 6) the time-varying bandwidth command shaping filter. In Sec. IV, simulation case studies are presented for 1) AOA tracking of step trajectories with constant EMA commands and with nominal and $\pm 50\%$ variations in the aerodynamic coefficients, 2) AOA tracking of sinusoidal trajectories with both constant and variable EMA commands and with nominal and $\pm 50\%$ variations in the aerodynamic coefficients, and 3) NA tracking of both step and sinusoidal trajectories using an AOA state observer. Section V concludes with a summary of the results and suggestions for further studies.

II. EMA Control by Direct Synthesis

The EMA synthesis control technique is exemplified here with a generic second-order LTV system

$$\ddot{y} + a_2(t)\dot{y} + a_1(t)y = u \tag{1}$$

This LTV system can be written in an operator form $\mathcal{D}_a\{y\} = u$, where

$$\begin{aligned}\mathcal{D}_a &= \mathrm{D}^2 + a_2(t)\mathrm{D} + a_1(t)\\ &= [\mathrm{D} - \lambda_2(t)][\mathrm{D} - \lambda_1(t)]\\ &= \mathrm{D}^2 - [\lambda_1(t) + \lambda_2(t)]\,\mathrm{D} + \lambda_1(t)\lambda_2(t) - \dot{\lambda}_1(t)\end{aligned} \tag{2}$$

is known as a polynomial differential operator and the factorization is known as Cauchy–Floquet factorization. The scalar functions $\lambda_1(t)$ and $\lambda_2(t)$ are called SD eigenvalues for the LTV system (1), and $\rho(t) = \lambda_1(t)$ is called a PD eigenvalue.[2] It follows from Eq. (2) that the SD eigenvalues satisfy a set of (nonlinear, differential) SD-characteristic equations

$$\begin{aligned}\dot{\lambda}_1(t) + \lambda_1^2(t) + a_2(t)\lambda_1(t) + a_1(t) = 0\\ \lambda_2(t) = -a_2(t) - \lambda_1(t)\end{aligned} \tag{3}$$

Note that, in general, the factors $[\mathrm{D} - \lambda_1(t)]$ and $[\mathrm{D} - \lambda_2(t)]$ are noncommutative and nonunique and $\lambda_1(t)$ and $\lambda_2(t)$ may be complex-valued functions. In the latter case, they form an affine complex-conjugate pair[2]

$$\lambda_1(t) = \sigma_1(t) + j\omega(t) \qquad \lambda_2(t) = \sigma_2(t) - j\omega(t) \tag{4}$$

where $\omega(t)$ satisfies

$$\dot{\omega} = [\sigma_2(t) - \sigma_1(t)]\omega \tag{5}$$

Now define the extended-mean (EM) value of an integrable function $\sigma(t)$ by

$$\mathrm{em}\{\sigma(t)\} = \limsup_{T \to \infty, t_0 \geq 0} \frac{1}{T}\int_{t_0}^{t_0+T} \sigma(\tau)\,\mathrm{d}\tau \tag{6}$$

Then the LTV system (1) with bounded piecewise smooth coefficients $a_1(t)$ is exponentially stable for all $t_0 \geq 0$ if $\mathcal{D}_a$ has a bounded SD spectrum $\{\lambda_1(t), \lambda_2(t)\}$ with EM values in the left half plane (LHP) of $\mathbb{C}$; i.e., for some $M > 0$,

$$|\lambda_i(t)| < M, \qquad \mathrm{em}\{\mathrm{Re}[\lambda_i(t)]\} < 0, \qquad i = 1, 2 \tag{7}$$

This statement follows from a necessary and sufficient criterion for exponential stability of a LTV system based on the EM of PD eigenvalues given in Ref. 10. For a second-order PDO, SD eigenvalues $\lambda_i(t)$ are related to PD eigenvalues $\rho_i(t)$ by $\lambda_1(t) = \rho_1(t)$, $\lambda_2(t) = \rho_2(t) + \dot{\omega}(t)/\omega(t)$, where $\omega(t) = \mathrm{Im}\{\rho_1(t)\}$ when $\rho_i(t)$ are complex conjugate, or $\omega(t) = [\rho_1(t) - \rho_2(t)]/2$ when $\rho_i(t)$ are real valued. In particular, $\mathrm{em}\{\mathrm{Re}\,[\lambda_i(t)]\} = \mathrm{em}\{\mathrm{Re}[\rho_i(t)]\}$ if $\lambda_i(t)$ are bounded, because then $\mathrm{em}\{\dot{\omega}(t)/\omega(t)\} = 0$. A necessary condition for bounded $\lambda_i(t)$ is that the coefficients $a_i(t)$ are bounded. Thus, if the LTV system (1) is unstable, a feedback control law

$$u(t) = k_1(t)y(t) + k_2(t)\dot{y}(t) \tag{8}$$

can be synthesized so that SD eigenvalues $\gamma_1(t)$ and $\gamma_2(t)$ of the closed-loop system $\mathcal{D}_h\{y\} = 0$, where

$$\begin{aligned}\mathcal{D}_h &= \mathrm{D}^2 + h_2(t)\mathrm{D} + h_1(t)\\ &= [\mathrm{D} - \gamma_2(t)][\mathrm{D} - \gamma_1(t)]\end{aligned} \tag{9}$$

has the desired EM values in the LHP of $\mathbb{C}$.

Now implementing the control law (8) on the LTV plant (1) and comparing coefficients with the desired closed-loop system (9) yield

$$h_i = a_i(t) - k_i(t) \tag{10}$$

Because $h_i(t)$ are related to $\gamma_i(t)$ by

$$h_1(t) = \gamma_1(t)\gamma_2(t) - \dot{\gamma}_1(t) \qquad h_2(t) = -[\gamma_1(t) + \gamma_2(t)] \tag{11}$$

the feedback control gains $k_i(t)$ can then be synthesized as

$$\begin{aligned}k_1(t) &= a_1(t) + \dot{\gamma}_1(t) - \gamma_1(t)\gamma_2(t)\\ k_2(t) &= a_2(t) + \gamma_1(t) + \gamma_2(t)\end{aligned} \tag{12}$$

Although the EM is defined as a limiting value as $t \to \infty$, in practice it suffices for exponential stability that the running average

$$C_i(t) = \frac{1}{t - t_0}\int_{t_0}^{t} \mathrm{Re}[\lambda_i(\tau)]\,\mathrm{d}\tau \leq -L < 0 \tag{13}$$

for some positive number L. This allows the "pole" locations to be reassigned to achieve optimum performance under different operating stages or conditions. The desired profiles $C_i(t)$ are hereafter referred to as the extended mean assignment command (EMAC).

III. EMA Autopilot Design

There are essentially two approaches to nonlinear tracking control via (local) linearization: 1) linearizing the plant about a fixed operating point and then designing a linear tracking controller and 2) linearizing the plant about a nominal (operating) trajectory and then designing a linear regulator to steer the linear state variables, which are tracking errors of the nonlinear system, to 0 exponentially. An advantage of the first approach is that the linearized model is independent of the tracking command trajectory, thereby allowing an LTI model if the nonlinear plant is autonomous (time invariant) in the first place. As a consequence, the vast well-developed LTI tracking control techniques can be employed to achieve the design goals. The main drawback of this approach is that to retain validity of the linearization, both the command and the output trajectories cannot deviate from the constant operating point too far, nor can it vary too fast. This requirement can be overly restrictive for many applications, such as the missile autopilot under consideration. A common practice to circumvent this restriction is by linearizing the plant at discrete operating points and switching in real time the linear tracking controllers for each operating point, i.e., gain scheduling, according to the command trajectory. In a case where the linearized model is time varying, either elaborate LTV design techniques must be employed for each linear tracking controller, or, as a common practice, ad hoc gain scheduling of LTI tracking controllers must be used to achieve stability and tracking.

In contrast, the second approach only requires that the output trajectory stay close to the command trajectory, which is the goal of tracking control to begin with. An added advantage is that only a linear regulator, instead of one or more linear tracking controllers, needs to be designed. Therefore, this approach allows tracking of fast time-varying command trajectories with large variations without real-time gain scheduling. With the EMA controller as the linear regulator for tracking error stabilization, it is natural to adopt this latter approach for the autopilot design task at hand. The missile pitch dynamics and the design of the EMA controller-based AOA and NA tracking controllers are discussed in Secs. III.A–III.C.

As an implementation issue, the second approach requires a nominal control to put the system output on the nominal trajectory. (The first approach also needs a nominal control, which consists of two parts: a nonlinear nominal control, which is a constant for an autonomous nonlinear plant but otherwise a time function, and a linear nominal control, which depends on the command trajectory and can be generated, in principle, from the inverse of the linearized model. This latter component is often disguised by linear tracking control techniques such as integral control or linear quadratic optimal tracking control.) The nominal control can, in principle, be generated from the inverse of the nonlinear plant. Because most physical systems, whether linear or nonlinear, are low-pass filters in nature, their exact inverses are either noncausal or, in the case of nonminimum phase zero dynamics, unstable. However, stable and physically realizable pseudoinverses may be constructed that approximate the inverse plant model to a satisfactory degree of accuracy within the operating bandwidth. Such a pseudoinverse is implemented for our autopilot using a static RBF NN, which is trained with constant trajectories within the specified operating range. It is noted that once an inverse model is implemented, the closed-loop system needs only the present and past values of the command trajectory; therefore, the command trajectories need not be known a priori. It is also remarked that the approximation error of the pseudoinverse plant model can be viewed as an exogenous disturbance signal, which, as long as it remains reasonably small, can be accommodated by the tracking error regulator. (The error is considered reasonably small so long as the disturbed output trajectory remains sufficiently close to the command trajectory so that the linearization remains valid. Exact error tolerance depends on the nonlinearity of the plant and the operating range of the system variables. Such a tolerance is often difficult to establish analytically, but can always be determined experimentally with a given confidence level. This should not be viewed as a restriction of the design approach, as locality is an inherent nature of nonlinear dynamics. In fact, this error tolerance can be surprisingly large for smooth nonlinearities.) Detailed information on the RBF-NN design and implementation is given in Sec. III.D.

A salient advantage of using LTV controllers/filters is that they can accomplish tasks and performances beyond the reach of LTI counterparts. To exemplify this advantage, Sec. III.E presents a time-varying EMA command that automatically reduces the controller gains when the target trajectory is too far away or has been acquired, thereby saving control energy while maintaining stability and good tracking performance. Another example is given in Sec. III.F, where a time-varying bandwidth command shaping filter is employed to eliminate the need for actuator position and rate limiters while maintaining good tracking of both abrupt and smooth command trajectories.

A. Dynamic Model of the Missile Airframe

Consider a hypothetical tail-controlled missile whose pitch-axis dynamics are described by

$$\begin{aligned}\dot{\alpha}(t) &= K_\alpha M(t) C_n[\alpha(t), \delta(t), M(t)]\cos[\alpha(t)] + q(t)\\ \dot{q}(t) &= K_q M^2(t) C_m[\alpha(t), \delta(t), M(t)]\\ \eta_z(t) &= K_z M^2(t) C_n[\alpha(t), \delta(t), M(t)]\end{aligned} \tag{14}$$

where

$$\begin{aligned}C_n[\alpha, \delta, M] &= a_n\alpha^3 + b_n\alpha|\alpha| + c_n(2 - M/3)\alpha + d_n\delta\\ C_m[\alpha, \delta, M] &= a_m\alpha^3 + b_m\alpha|\alpha| + c_m(-7 + 8M/3)\alpha + d_m\delta\end{aligned} \tag{15}$$

The tail-fin actuator dynamics are described by

$$\frac{\mathrm{d}}{\mathrm{d}t}\begin{bmatrix}\delta(t)\\ \dot{\delta}(t)\end{bmatrix} = \begin{bmatrix}0 & 1\\ -\omega_a^2 & -2\zeta\omega_a\end{bmatrix}\begin{bmatrix}\delta(t)\\ \dot{\delta}(t)\end{bmatrix} + \begin{bmatrix}0\\ \omega_a^2\end{bmatrix}\delta_c(t) \tag{16}$$

The values of the various constant parameters in the dynamic equations (14–16) can be found in Refs. 5–7, where this missile model has been used as a benchmark for nonlinear gain-scheduling design techniques.

B. AOA Tracking Subsystem

At this initial stage, we simplify the problem by neglecting the actuator dynamics, assuming its bandwidth is sufficiently wide. Let

$$\boldsymbol{\xi}(t) = \begin{bmatrix}\xi_1(t)\\ \xi_2(t)\end{bmatrix} = \begin{bmatrix}\alpha(t)\\ q(t)\end{bmatrix} \tag{17}$$

be the state vector of the reduced-order nonlinear model. Then the state equation is given by

$$\dot{\boldsymbol{\xi}} = \boldsymbol{f}(\boldsymbol{\xi}, \delta) = \begin{bmatrix}f_1(\xi_1, \xi_2, \delta)\\ f_2(\xi_1, \xi_2, \delta)\end{bmatrix} \qquad \eta_z = g(\boldsymbol{\xi}, \delta) = g(\xi_1, \xi_2, \delta) \tag{18}$$

where

$$\begin{aligned}f_1(\xi_1, \xi_2, \delta) &= K_\alpha M C_n(\xi_1, \delta, M)\cos(\xi_1) + \xi_2\\ f_2(\xi_1, \xi_2, \delta) &= K_q M^2 C_m(\xi_1, \delta, M)\\ g(\xi_1, \xi_2, \delta) &= K_z M^2 C_n(\xi_1, \delta, M)\end{aligned}$$

Now for a given commanded normal acceleration profile $\eta_c(t)$, let $\bar{\delta}(t)$ be the nominal tail-fin deflection and $\bar{\boldsymbol{\xi}}(t)$ be the nominal state trajectory such that

$$\dot{\bar{\boldsymbol{\xi}}}(t) = \boldsymbol{f}[\bar{\boldsymbol{\xi}}(t), \bar{\delta}(t)] \qquad \eta_c(t) = g[\bar{\boldsymbol{\xi}}(t), \bar{\delta}(t)] \tag{19}$$

Define the tracking errors by

$$\boldsymbol{x}(t) = \boldsymbol{\xi}(t) - \bar{\boldsymbol{\xi}}(t) \qquad y(t) = \eta_z(t) - \eta_c(t) \tag{20}$$

and the tracking error control input by

$$v(t) = \delta(t) - \bar{\delta}(t) \tag{21}$$

Then the linearized tracking error dynamics are given by

$$\dot{\boldsymbol{x}} = \boldsymbol{A}(t)\boldsymbol{x} + \boldsymbol{B}(t)v \qquad y = \boldsymbol{C}(t)\boldsymbol{x} + \boldsymbol{D}(t)v \tag{22}$$

where

$$\boldsymbol{A}(t) = \left.\frac{\partial \boldsymbol{f}}{\partial \boldsymbol{\xi}}\right|_{\bar{\xi},\bar{\delta}} = \begin{bmatrix} a_{11}(t) & 1 \\ a_{21}(t) & 0 \end{bmatrix} \tag{23}$$

with

$$a_{11}(t) = K_\alpha M(t)\Big(\Big\{3a_n\bar{\xi}_1^2(t) + 2b_n\big|\bar{\xi}_1(t)\big| + c_n[2 - M(t)/3]\Big\} \times \cos[\bar{\xi}_1(t)] - \Big\{a_n\bar{\xi}_1^3(t) + b_n|\bar{\xi}_1(t)|\bar{\xi}_1(t) + c_n[2 - M(t)/3]\bar{\xi}_1(t) + d_n\bar{\delta}\Big\}\sin[\bar{\xi}_1(t)]\Big)$$

$$a_{21}(t) = K_q M^2(t)\Big\{3a_m\bar{\xi}_1^2(t) + 2b_m|\bar{\xi}_1(t)| + c_m[-7 + 8M(t)/3]\Big\}$$

$$\boldsymbol{B}(t) = \left.\frac{\partial \boldsymbol{f}}{\partial \delta}\right|_{\bar{\xi},\bar{\delta}} = \begin{bmatrix} b_1(t) \\ b_2(t) \end{bmatrix} = \begin{bmatrix} K_\alpha M(t) d_n \cos[\bar{\xi}_1(t)] \\ K_q d_m M^2(t) \end{bmatrix} \tag{24}$$

$$\boldsymbol{C}(t) = \left.\frac{\partial g}{\partial \boldsymbol{\xi}}\right|_{\bar{\xi},\bar{\delta}} = [c_1(t) \quad 0] \tag{25}$$

with

$$c_1(t) = K_z M^2(t)\Big\{3a_n\bar{\xi}_1^2(t) + 2b_n|\bar{\xi}_1(t)| + c_n[2 - M(t)/3]\Big\}$$

$$\boldsymbol{D}(t) = \left.\frac{\partial g}{\partial \delta}\right|_{\bar{\xi},\bar{\delta}} = \big[d_n K_z M^2(t)\big] \tag{26}$$

A nonlinear tracking controller based on this linearization technique consists of an inverse of the input/output (I/O) map $\delta \mapsto \eta_z$, which implements the nominal control $\bar{\delta}$ given a desired trajectory η_c, and a tracking error stabilization controller, which drives the tracking errors $\boldsymbol{x}(t)$ and $y(t)$ to zero exponentially as $t \to \infty$.

For the I/O map to be invertable, its zero dynamics must be of minimum phase. This is the case for AOA I/O map $\delta \mapsto \alpha$. Otherwise, as for the NA I/O map $\delta \mapsto \eta_z$, exact tracking will not be feasible, but good tracking performance with tolerable errors is still attainable if a stable approximation to the inverse I/O map is used in conjunction with an exponentially stable tracking error controller.

Assuming a stable approximation to the inverse I/O map is available, the autopilot design task amounts to finding a control law such that $y(t) \to 0$ exponentially for any admissible normal acceleration profile $\eta_c(t)$. This can be achieved using an EMA controller. However, to use the prototype EMA controller, it is necessary to transform the linearized tracking error dynamics into the phase-variable canonical form. This can be done via Silverman's coordinate transformation, provided that $[\boldsymbol{A}, \boldsymbol{B}]$ is uniformly completely controllable. Whereas this approach will result in a minimal realization, the resulting system coefficients are very complicated. To simplify the matter, here we opt to a nonminimal realization that yields a phase-variable canonical form with very simple coefficients. However, in so doing one must ensure that the uncontrollable internal mode be exponentially stable.

To that end, apply the state coordinate transformation

$$\boldsymbol{x} = \boldsymbol{L}(t)\boldsymbol{z} \tag{27}$$

where $L(t)$ is a (time-varying) coordinate transformation matrix given by

$$\boldsymbol{L}(t) = \begin{bmatrix} 1 & 0 \\ -a_{11}(t) & 1 \end{bmatrix} \tag{28}$$

Then the linearized system (22) in the z coordinates becomes

$$\dot{\boldsymbol{z}} = \boldsymbol{A}_c(t)\boldsymbol{z} + \boldsymbol{B}_c(t)v \qquad y = \boldsymbol{C}_c(t)\boldsymbol{z} + \boldsymbol{D}_c(t)v \tag{29}$$

where $\boldsymbol{A}_c(t) = \boldsymbol{L}^{-1}(t)[\boldsymbol{A}(t)\boldsymbol{L}(t) - \dot{\boldsymbol{L}}(t)]$ is of the companion form

$$\boldsymbol{A}_c(t) = \begin{bmatrix} 0 & 1 \\ -a_1(t) & -a_2(t) \end{bmatrix} = \begin{bmatrix} 0 & 1 \\ \dot{a}_{11}(t) + a_{21}(t) & a_{11}(t) \end{bmatrix}$$

$$\boldsymbol{B}_c(t) = \boldsymbol{L}^{-1}(t)\boldsymbol{B}(t) = \begin{bmatrix} b_1(t) \\ a_{11}b_1(t) + b_2(t) \end{bmatrix}$$

$$\boldsymbol{C}_c(t) = \boldsymbol{C}(t)\boldsymbol{L}(t) = \boldsymbol{C}(t) \qquad \boldsymbol{D}_c(t) = \boldsymbol{D}(t)$$

Note that $z_1(t) = x_1(t) = \alpha(t) - \bar{\alpha}(t)$. By eliminating z_2 from Eq. (29), it is seen that this state equation is equivalent to a scalar equation

$$\ddot{z}_1 + a_2(t)\dot{z}_1 + a_1(t)z_1 = b_1(t)\dot{v} + [b_2 + \dot{b}_1(t)]v \tag{30}$$

To render this equation into the phase-variable form, we introduce the AOA zero dynamics

$$\dot{v} + \{[b_2(t) + \dot{b}_1(t)]/b_1(t)\}v = [1/b_1(t)]u \tag{31}$$

Combining Eqs. (30) and (31) yields the desired form

$$\ddot{z}_1 + a_2(t)\dot{z}_1 + a_1(t)z_1 = u \tag{32}$$

Note that $v(t)$ is now a hidden state in the augmented system $u \mapsto z_1$. The zero of AOA dynamics in the augmented system has been canceled by its inverse. To make the cancellation valid, we need verify that the zero dynamics is exponentially stable. This is indeed the case because it is readily verified that the SD eigenvalue

$$\lambda_z(t) = -\frac{b_2(t) + \dot{b}_1(t)}{b_1(t)} \tag{33}$$

for Eq. (31) has a negative EM for all $|\alpha(t)| < \pi/2$ and $2\,M(t) > 0$.

Now an EMA control law $u(t)$ can be designed for the AOA tracking error dynamics (32) using the standard procedure outlined in Sec. II. The overall closed-loop system implementation is shown in Fig. 1.

C. AOA Observer for NA Tracking System

The missile guidance system typically generates a NA command profile. To take advantage of the minimum phase zero dynamics in AOA, and the LTV model (32) for AOA dynamics that is readily controlled by the EMA technique, the (nonminimum phase) NA tracking is achieved via an AOA tracking subsystem shown in Fig. 1. Because NA is related to AOA and the tail-fin deflection via a nonlinear algebraic mapping it is natural to design a nonlinear time-varying state observer that estimates the AOA error from the measurement of the NA error, as shown in Fig. 2. This is accomplished by inverting the linearized output error equation (25). A low-pass filtered

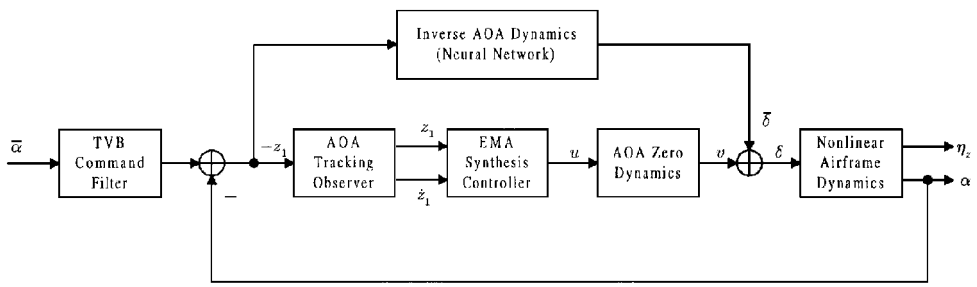

Fig. 1 AOA tracking subsystem.

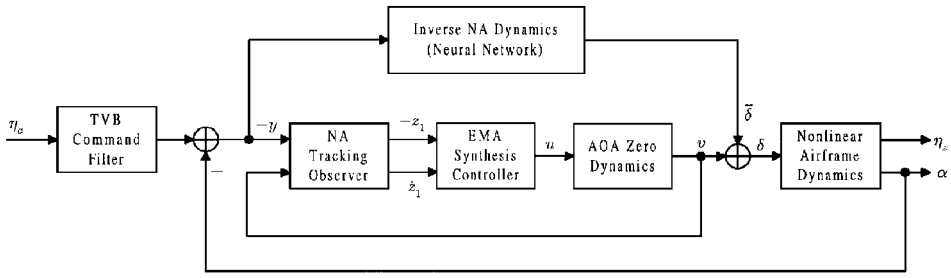

Fig. 2 NA tracking subsystem.

differentiator with a transfer function $200s/(s + 200)$ is used to estimate the AOA error rate. It is noted that the observer performance could be improved by using a static NN to approximate the nonlinear relation between the NA and AOA errors. Other ways of implementing the observer were discussed in Ref. 1.

It is noted that this NA tracking strategy circumvents the nonminimum phase problem of NA tracking implicitly and yields good results when the mapping between the NA and AOA errors is accurate. This method is applicable to other nonminimum phase tracking problems and may be termed algebraic output redefinition, as opposed to the (dynamic) output redefinition method proposed in Ref. 8.

D. NN-Based Dynamic Inverse

Nonlinear tracking by linearization along a nominal trajectory calls for an inverse model of the plant I/O dynamics to generate the required nominal control input. It is well known that when the plant has nonminimum phase zero dynamics, such as the case of NA tracking, the inverse model is unstable. Consequently, perfect tracking is not possible. However, if the plant is stable, it is possible to find the inverse for constant input and output trajectories. This static inverse mapping can be used as an approximation of the (unstable) inverse plant model. Variable command trajectories can be approximated by piecewise constant trajectories for which exact nominal control can be generated by the static inverse plant model. The discrepancy is then compensated for by the tracking error controller, provided that the error is sufficiently small so that the linearization remains valid.

The nominal control $\bar{\delta}$ for a constant command trajectory is implemented by a static RBF NN. One NN is used in the system shown in Fig. 1 for AOA command $\bar{\alpha}$, and another one is used in the system shown in Fig. 2 for NA command η_c. The training data for the network were acquired from the MATLAB function trim, which locates the equilibrium points of the missile model, i.e., the nominal tail fin deflection required to achieve the desired output (AOA or NA). These data were then used to train an RBF NN via the MATLAB function solverb. The training of a RBF NN with some 200 neurons required an order of 10^{10} floating point operations per second (flops) using the Unix version Neural Networks Toolbox Version 2.0 for MATLAB. The error surface between the desired inverse mapping of $\bar{\alpha} \mapsto \bar{\delta}$ and a 200 neuron RBF NN implementation is plotted in Fig. 3, where it can be seen that, except at a few peripheral points outside the operating range, the errors are below 0.5 deg. This error magnitude is readily accommodated by the EMA tracking controller.

It is noted that, in practice, training data can be obtained directly from wind-tunnel or flight tests thereby bypassing the inversion of an analytical dynamic model that is obtained from the same sets of data. Another advantage of the RBF NN implementation of the inverse plant model is that, owing to the localization of its receptive fields and the small number of weights, in-flight learning of a particular missile's aerodynamics can be facilitated using prior generic off-line training as the initial states. This will greatly increase the accuracy and robustness of the overall tracking system in the presence of parameter uncertainties.

E. Time-Varying EMAC

As the closed-loop stability is guaranteed by the extended-mean stability criterion, the EMAC $C_i(t)$ in the EMA controller need not be constant, as long as they stay in the LHP of $\mathbb{C}$. This feature may

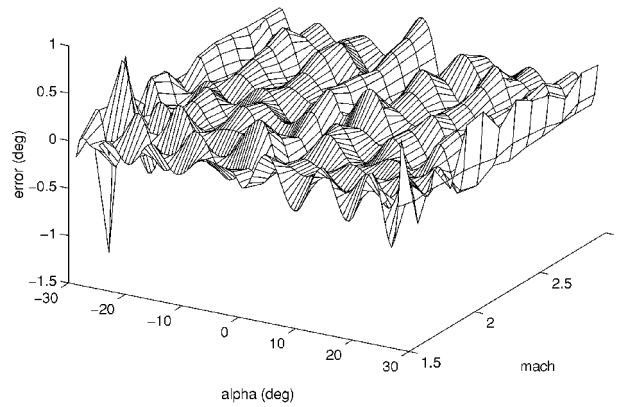

Fig. 3 NN error surface.

be advantageous, for instance, in cases where control energy is a prime concern and performance may be sacrificed during noncritical maneuverings. To exemplify this concept, a variable EMAC logic is defined as follows:

$$C_i(t) = C_{i0} + g[\epsilon(t)/\epsilon_0] \exp[-\epsilon(t)/\epsilon_0] \tag{34}$$

where $\epsilon(t)$ is the tracking error, ϵ_0 is a predetermined tracking error threshold, C_{i0} is the minimum EMAC, and g is a design constant that, when added to C_{i0}, determines the maximum EMAC. This EMAC logic generates the maximum EMAC when the tracking error $\epsilon(t)$ is equal to ϵ_0 and reduces to the minimum EMAC when $\epsilon(t)$ is either zero or infinity. Therefore, it reduces control energy when the tracking has been acquired, or when the desired trajectory is still far away to avoid unnecessary maneuvering. It also helps to reduce overshoot as the control gains reduce as tracking is being acquired. This EMAC logic was implemented and tested in the simulation studies presented in Sec. IV.

F. Time-Varying Bandwidth Command Shaping Filter

In practice, fast tracking performance is always constrained by the physical limit of the actuator rate. A common practice in coping with this dilemma is to use an actuator rate limiter. A major drawback of this method is that the system becomes unpredictable when the actuator rate is saturated. It may result in limit cycles, or even in instability.

An alternative approach is to use a tracking command filter. The filter should greatly reduce the acceleration and rate of an abrupt command trajectory, whereas it should have little effect on smooth trajectories that can be tracked within the actuator limits. These two requirements cannot be achieved with a fixed-parameter filter. For instance, the AOA tracking subsystem can track a 0.5 Hz, 17.18-deg amplitude sine wave within the 500 deg/s actuator rate limits without any command shaping. However, without command shaping, the same system tracks a step command of 17.18-deg magnitude with a settling time of less than 0.2 s, but requires a maximum actuator rate of 76,200 deg/s. When a third-order LTI Bessel filter with a bandwidth $\omega_n = 10$ is applied to the step tracking command, the actuator rate is reduced to within the limits with a satisfactory tracking performance, but the sinusoidal tracking then has an unnecessary tracking delay of 0.25 s, or a 45-deg phase lag.

Taking advantage of the EM stability criterion, a novel second-order LTV filter with a variable bandwidth was designed to deal

with the conflicting requirements for a command shaping filter. The governing equation for the filter is given by

$$\ddot{c}_{\text{out}} + [2\zeta\omega_n(t) - \dot{\omega}_n(t)/\omega_n(t)]\dot{c}_{\text{out}} + \omega_n^2(t)c_{\text{out}} = c_{\text{in}} \qquad (35)$$

where ζ is a constant damping coefficient and $\omega_n(t) > 0$ determine the effective bandwidth. When $\omega_n(t) \equiv$ const, this filter reduces to the well-known second-order LTI low-pass filter. Details on the design are given in a separate paper[10] (see also Ref. 1), where convincing simulation results are also given to show how the time-varying bandwidth (TVB) filter functions automatically as a second-order low-pass LTI filter with bandwidth $BW = 100$ when the command is a smooth sinusoidal waveform, whereas as a third-order LTI Bessel filter with $BW = 10$ when the command is an abrupt step function. The TVB filter is implemented in both the AOA and NA tracking systems shown in Figs. 1 and 2.

IV. Simulation Case Studies

Simulation studies were performed to validate the design using a priori unknown command trajectories. The plant model used in the simulations includes the actuator dynamics (16). The TVB command shaping filter was used for all of the cases, so that no actuator amplitude or rate limiter was needed for command tracking.

Case 1: AOA Step Trajectory Tracking

The AOA EMA control provides remarkable results for step command tracking. Figure 4 displays a 3-s piecewise constant AOA tracking command, the TVB filtered command, and the AOA output. It also contains the response without using the TVB filter, where the EMA controller accurately tracks step commands with a settling time less than 0.2 s, but the actuator rate reached 76,200 deg/s. With the TVB filter the actuator rate was well within the specified limit of 500 deg/s (cf. Refs. 1 and 11). The output tail deflection is also limited, but this limit was never even approached during simulation. Figure 5 shows simulation results for the four possible combinations of $\pm 50\%$ variations in the two aerodynamic coefficients $C_n(t)$ and $C_m(t)$, indicating excellent robustness of the closed-loop system.

Case 2: AOA Variable Trajectory Tracking

Although the NN was trained to generate a nominal control input only for static or step commands, the proposed controller configuration can track arbitrary trajectories because of the EMA section's ability to accommodate errors in the nominal control input. Also, the EMAC need not be a constant. To demonstrate these points, in this case study an unreasonably demanding sinusoidal AOA command trajectory is to be tracked by the autopilot without any tuning or scheduling of the controller parameters as used in case 1. Figures 6–10 compare the results for TVB filtered sinusoidal tracking with both constant and variable EMAC. Shown together in Fig. 6 are the AOA tracking command, the TVB filtered command, and the AOA output with constant EMAC at 20 and with variable EMAC between

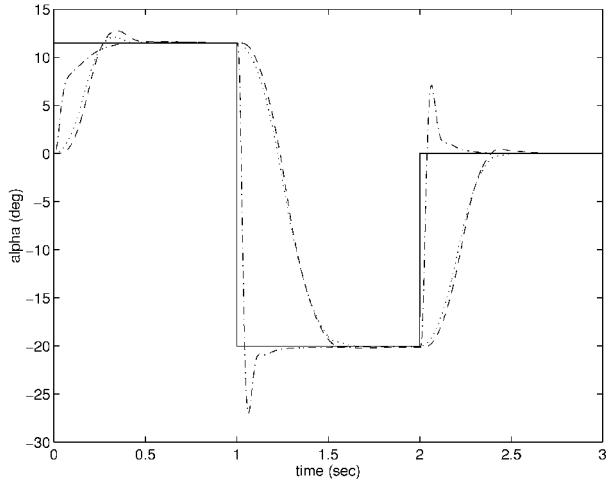

Fig. 4 AOA step trajectory tracking performance: ——, AOA command; ·····, TVB filtered command; – – –, AOA output; and – · –, AOA without command filter.

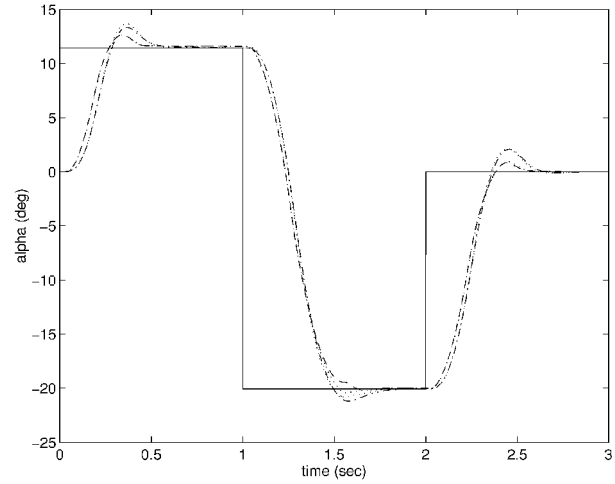

Fig. 5 Robustness test; ±50% variation on C_m and C_n: ——, AOA command; ·····, +50% C_m, +50% C_n; – – –, +50% C_m, − 50% C_n; – · –, − 50% C_m, +50% C_n; and ·····, − 50% C_m, − 50% C_n.

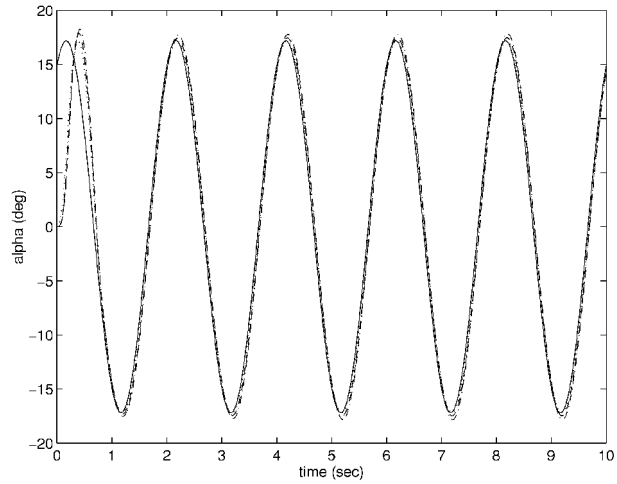

Fig. 6 AOA sinusoidal trajectory tracking performance: ——, AOA command; ·····, TVB filtered command; – – –, constant EMAC; and – · –, variable EMAC.

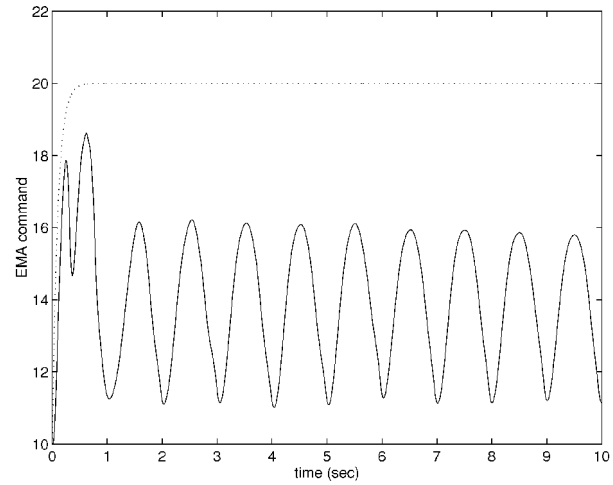

Fig. 7 Constant vs variation EMAC: ——, variable EMA command and ·····, constant EMA command.

10 and 20 as defined in Eq. (34). It clearly shows the remarkable tracking performance. The filtered command has very little magnitude dampening and phase change, demonstrating how little effect the TVB filter has on a smooth trajectory comparing to its effect on the step command in the preceding case.

Shown in Fig. 7 are the constant and variable EMAC. It can be seen that the variable EMAC indeed increases toward the maximum

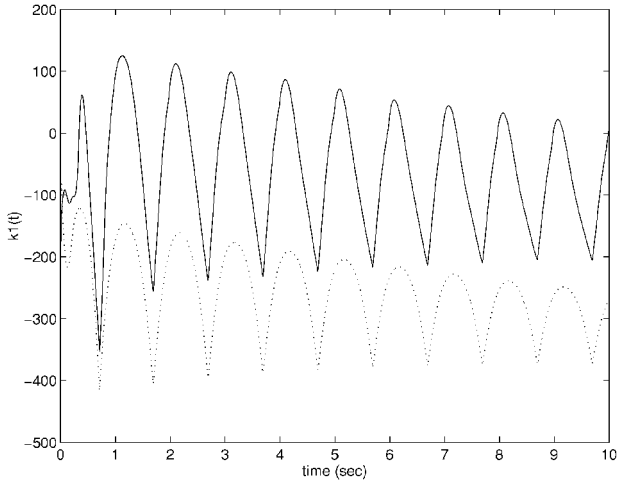

Fig. 8 Feedback gain $k_1(t)$:——, variable EMA command and ·····, constant EMA command.

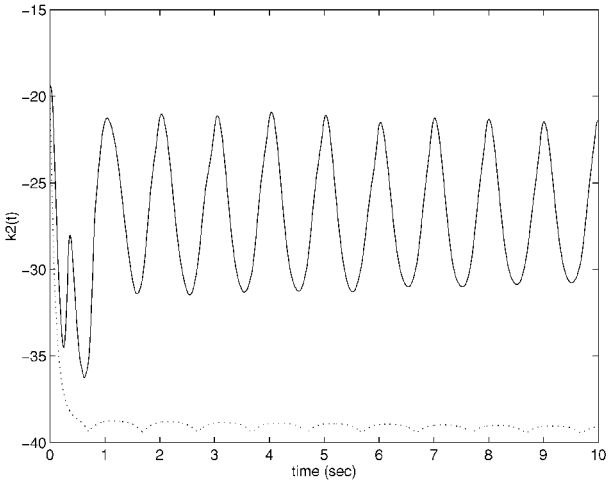

Fig. 9 Feedback gain $k_2(t)$: ——, variable EMA command and ·····, constant EMA command.

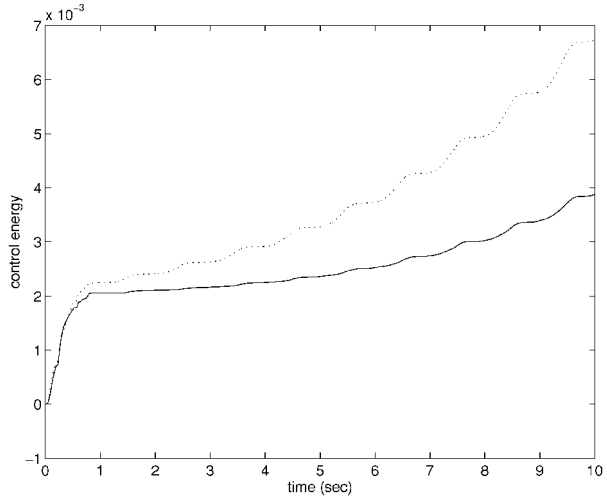

Fig. 10 Tracking error control energy: ——, variable EMA command and ·····, constant EMA command.

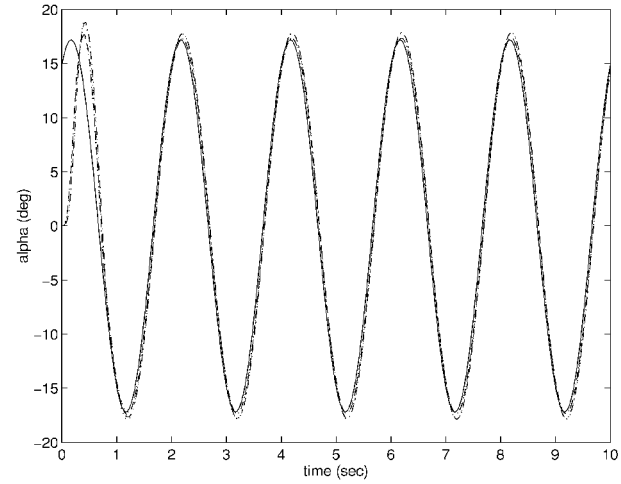

Fig. 11 Robustness test; ±50% variation on C_m and C_n: ——, AOA command; ·····, +50% C_m, +50% C_n; – – –, +50% C_m, −50% C_n; – · –, −50% C_m, +50% C_n; and ·····, −50% C_m, −50% C_n.

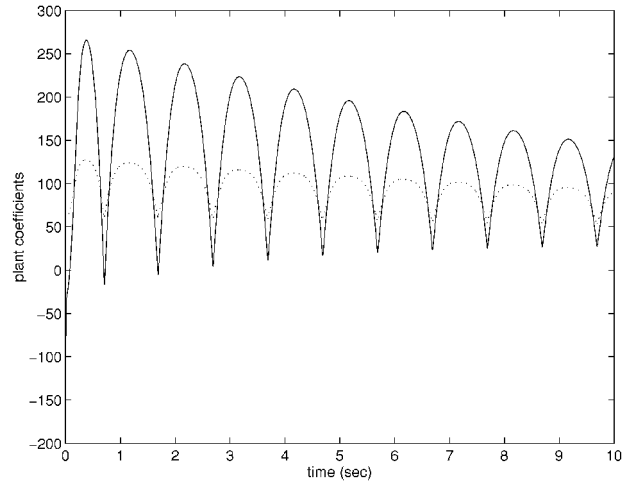

Fig. 12 Time-varying plant coefficients $a_1(t)$ and $100 \cdot a_2(t)$: ——, $a_1(t)$ and ·····, $100 \cdot a_2(t)$.

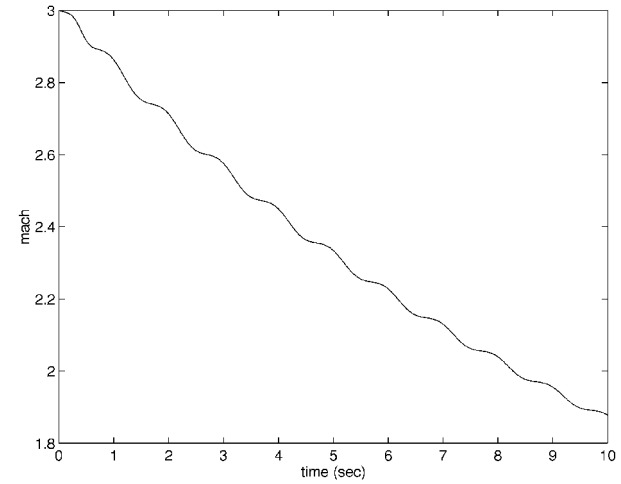

Fig. 13 Mach profile.

level of 20 when there is need for strenuous control action. Figures 8 and 9 show the corresponding feedback gains $k_1(t)$ and $k_2(t)$, respectively, for both constant and variable EMAC. The tracking performance under constant and variable EMAC are almost indistinguishable in Fig. 6, but in a long run the latter indeed saves control energy, as shown in Fig. 10, where the energy level is indicated by the integral of $\delta^2(t)$.

As in the first case, the robustness of the closed-loop system was tested for the constant EMA commands under all four possible combinations of ±50% error in the two aerodynamic coefficients $C_n(t)$ and $C_m(t)$. The results are again very good, as shown in Fig. 11.

Finally, the time-varying coefficients $a_1(t)$ and $a_2(t)$ in the linearized AOA error dynamics (30), and the Mach profile $M(t)$ as an important source of the time varying coefficients in the pitch airframe model are shown in Figs. 12 and 13 for the constant EMAC simulation. It is notable that Mach varies from 3.0 to 1.9, $a_1(t)$ between −153 and 266, and $a_2(t)$ between 0.52 and 1.27, during the 10-s sinusoidal AOA maneuvering and in the presence of ±50%

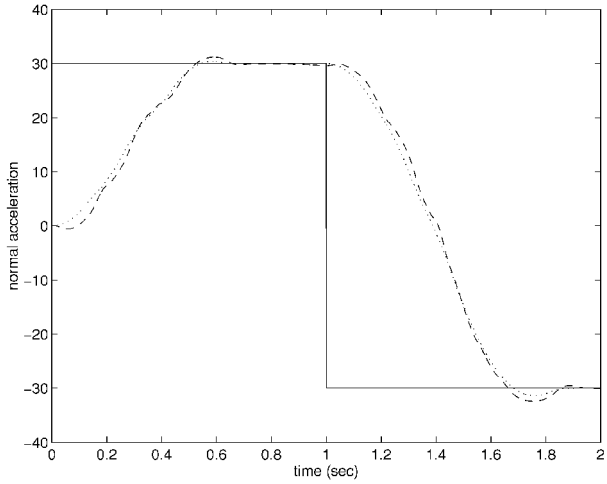

Fig. 14 NA step trajectory tracking performance: ——, NA command; ·····, TVB filtered NA command; and – – –, NA output.

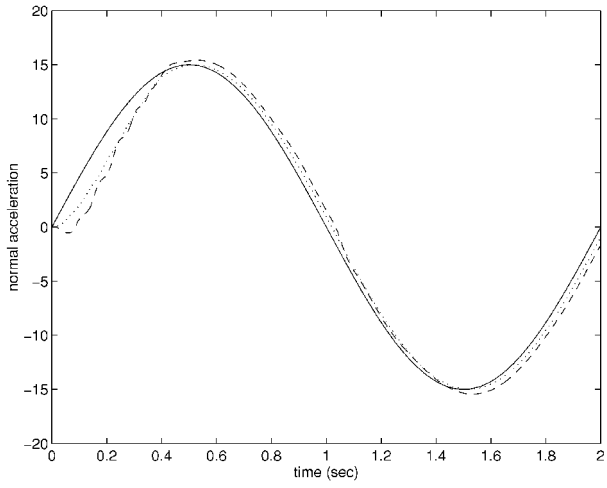

Fig. 15 NA sinusoidal trajectory tracking: ——, NA command; ·····, TVB filtered NA command; and – – –, NA output.

parameter variation. Moreover, the rates for the parameter variations are $-1612 < \dot{a}_1(t) < 1543$ and $-4.54 < \dot{a}_2(t) < 4.15$. The system is apparently not a slowly time-varying one. It is significant that no constant design parameters need to be scheduled for the entire operating range.

Case 3: NA Tracking Using AOA State Observer

Because in this case the NA tracking is achieved via a nonlinear algebraic mapping to the AOA tracking, we show in Figs. 14 and 15 only the NA tracking performance results for a step and sine trajectory, respectively. Each figure shows the NA command, the TVB filtered command, and the NA output. Although no design effort was explicitly directed to the nonminimum phase behavior of the NA tracking, the performances in both cases are remarkable. It was noted during the simulation studies that the NA tracking was very sensitive to variations in the acceleration (curvature) of the tracking command. Thus, the performance can be further improved by fine tuning the TVB command logic, which caused some curvature fluctuation in the filtered command.

V. Summary and Conclusions

We have presented the design and simulation study of a missile AOA and NA tracking autopilot using a recently developed EMA control technique. A radical departure from the conventional design philosophy is that nonlinearity and time variance of the dynamical system are not treated as nuisances. They are exploited purposely to accomplish design objectives beyond the reach of linear time-invariant control techniques. Salient features of the EMA autopilot include 1) good tracking performance for arbitrary trajectories without scheduling of any constant design parameters throughout the entire Mach operating range, 2) time-varying EMA control gains to improve tracking performance, 3) implementation of the inverse pitch dynamics using a static NN, and 4) a TVB command shaping filter that effectively reduces the actuator rate while maintaining good tracking response for both smooth and abrupt trajectories. Simulation results have shown that the EMA control technique, though still in its embryonic stage, has become a viable design tool for realistic control problems.

Acknowledgments

The authors gratefully acknowledge the U.S. Air Force Office of Scientific Research Summer Faculty Research/Graduate Student Program sponsored by the Bolling Air Force Base, Washington, D.C., and the U.S. Air Force Wright Laboratory, Eglin Air Force Base, Florida, for financial support during this research. The second author also expresses his heartfelt appreciation for financial support from the State of Louisiana via the Board of Regents' Dean's Fellowship in Engineering. The authors sincerely thank J. Cloutier, C. Mracek, J. Evers, and R. Zachery for their inspiration and valuable discussions during this work, and the editor and reviewers for their valuable suggestions for improving this paper.

References

[1]Zhu, J., and Mickle, M. C., "Missile Autopilot Design Based on a Unified Spectral Theory for Linear Time-Varying Systems," *Final Report for the 1995 AFOSR Summer Faculty Research Program*, U.S. Air Force Office of Scientific Research, Bolling AFB, Washington, DC, 1995, pp. 64-1–64-20.

[2]Zhu, J., "A Unified Spectral Theory for Linear Time-Varying Systems—Progress and Challenges," *Proceedings of the 34th IEEE Conference on Decision and Control* (New Orleans, LA), IEEE Control System Society, Piscataway, NJ, 1995, pp. 2540–2546.

[3]Zhu, J., and Johnson, C. D., "Unified Canonical Forms for Matrices over a Differential Ring," *Linear Algebra and Its Applications*, Vol. 147, March 1991, pp. 201–248.

[4]Zhu, J., and Xiao, W., "Intelligent Control of Time-Varying Dynamical Systems Using CMAC Artificial Neural Network," *Mathematical and Computer Modeling* (Special Issue on Neural Networks), Vol. 21, No. 1/2, 1995, pp. 89–107.

[5]White, D. P., Wozniak, J. G., and Lawrence, D. A., "Missile Autopilot Design Using a Gain Scheduling Technique," *Proceedings of the 26th IEEE Southeastern Symposium on Systems Theory* (Baton Rouge, LA), IEEE Computer Society Press, Los Alamitos, CA, 1994, pp. 606–610.

[6]Lawrence, D. A., and Rugh, W. J., "Gain Scheduling Dynamic Linear Controllers for a Nonlinear Plant," *Proceedings of the 32nd IEEE Conference on Decision and Control* (San Antonio, TX), IEEE Control System Society, Piscataway, NJ, 1993, pp. 1024–1029.

[7]Nichols, R. A., Reichert, R. T., and Rugh, W. J., "Gain Scheduling for H-Infinity Controllers: A Flight Control Example," *IEEE Transactions on Control Systems Technology*, Vol. 1, No. 2, 1993, pp. 69–79.

[8]Gopalswamy, S., and Hedrick, J. K., "Control of a High Performance Aircraft with Unacceptable Zerodynamics," *Proceedings 1992 American Control Conference* (Chicago, IL), American Automatic Control Council, Piscataway, NJ, 1992, pp. 1834–1838.

[9]Tsakalis, S. K., and Ioanou, P. A., *Linear Time-Varying Systems, Control and Adaptation*, Prentice–Hall, Englewood Cliffs, NJ, 1993, Chap. 5.

[10]Zhu, J., "A Necessary and Sufficient Stability Criterion for Linear Time-Varying Systems," *Proceedings of the 28th IEEE Southeastern Symposium on Systems Theory* (Baton Rouge, LA), IEEE Computer Society Press, Los Alamitos, CA, 1996, pp. 113–119.

[11]Zhu, J., and Mickle, M. C., "A Time-Varying Bandwidth Filter," *IEEE Transactions on Control Systems Technology* (submitted for publication).